Polyhedron 49 (2013) 84–92

Contents lists available at SciVerse ScienceDirect

Polyhedron

journal homepage: www.elsevier.com/locate/poly

Oxidation of carbohydrates of biological importance by the aquachromium(IV) ion

Juan Carlos González, María Florencia Mangiameli, Agostina Crotta Asis, Sebastián Bellú, Luis F. Sala *

Área Química General, Departamento de Químico-Física, Facultad de Ciencias Bioquímicas y Farmacéuticas, Universidad Nacional de Rosario, Suipacha 531, 2000 Rosario, Santa Fe, Argentina

ARTICLE INFO

Article history:
Received 17 August 2012
Accepted 25 September 2012
Available online 4 October 2012

Keywords:
$Cr^{IV}O^{2+}$
Saccharides
Kinetic

ABSTRACT

The oxidation reactions kinetics of a series of related saccharides by aqua-oxo chromium(IV) ion, $(H_2O)_5Cr^{IV}O^{2+}$, were carried out in perchloric acid aqueous solutions. These reactions yield superoxochromium(III) ion, CrO_2^{2+}, providing evidence that the two-electron reduction of CrO^{2+} to Cr^{2+} occurred in a single step. In all of these reactions, Cr^{2+} is the immediate product and could be trapped as CrO_2^{2+} when an excess of oxygen was present. The bimolecular rate constants for different aldoses and D-glucitol are independent of $[H^+]$ in the range 0.1–1.0 M. Relative reactivities of these saccharides toward CrO^{2+} reduction are 1-methyl-α-D-glucopyranose << 1-methyl-α-D-galactopyranose ~ 3-*O*-methyl-D-glucopyranose ~ 6-desoxi-L-galactopyranose ~ 2-desoxi-D-glucopyranose ~ D-glucopyranose << D-galactopyranose << D-glucitol. The oxidation of aldonic acid such as D-gluconic by CrO^{2+} showed the same mechanism but the redox process is strongly inhibited when $[H^+]$ increases. Activation parameters were also determined for selected reactions. On the basis of the kinetic result, activation parameters data and oxidized organic products, the mechanism of saccharides oxidation by CrO^{2+} is proposed to be a direct hydride-ion transfer.

1. Introduction

As been widely demonstrated, Cr^{VI} and its derivate compounds are important pollutants because of their mammalian toxicity and carcinogenicity [1–17].

The interaction of $Cr^{VI/V/IV}$ with different carbohydrates – low-weight neutral [16–26] and acid [26–30] molecules – which are present in biological systems has been demonstrated in previous studies. Carbohydrate and organic compounds with 2-hydroxy-carboxylate and/or *vic*-diolate functional groups are capable of chelating $Cr^{V/IV}$; as a result, they become suitable ligands for intracellular stabilization of these chromium oxidation states. It is known that both Cr^{IV} and Cr^{V} species can be formed intracellularly by reduction of Cr^{VI} [31] as well as by oxidation of Cr^{III} with the activated oxygen formed in enzymatic reactions [32]. Unlike Cr^{IV}, the Cr^{V} [33] species have extensively proved its ability to form complexes [26,29,30,34] of relative stability with biological substrates such as carbohydrates. Due to Cr^{IV} instability in aqueous media, some authors have stated for several years that this species does not have any aqueous solution chemistry [35]. The observation that Cr^{IV} does not form complexes of significant stability with 1,2-diol moieties of carbohydrates in neutral aqueous media was an argument against this species role in genotoxicity. However, in the last years, many authors have showed that this species can be stabilized by several organic substrates in acid aqueous media at pH 2–4 [10,29,30,34,36,37]. These acid conditions can be found in certain cellular vacuoles like lysosomes and phagosomes, where Cr^{VI} compounds are solubilized for their intake, generating intermediate oxidation states which play an important role in chromium genotoxicity [10,31,36].

Some authors established that Cr^{IV}-complexes with carboxylic ligands like oxalic, malonic, picolinic or quinic acids [38] are being produced in slightly acidic media and could be responsible for Cr^{IV} toxicity. The Cr^{IV} complexes lifetimes are shorter [38] than those of Cr^{V}, but show a higher reactivity in oxidation reactions due to higher redox potential [5]. Intracellular concentrations of Cr^{IV} complexes [39,40] are lower, compared with Cr^{V} complexes. Cr^{IV}-2-Hydroxy carboxylate bischelates have a higher capacity to lose one ligand molecule than their Cr^{V} analogs [38]. This means that Cr^{IV}-complexes can be favored in reactions with DNA. These chemical properties of Cr^{IV} and its complexes in aqueous solutions make probable candidates for the active species in Cr-induced genotoxicity. In the literature it has been reported that Cr^{IV} is a more potent DNA damaging agent than Cr^{V}. These results are not definitive because no data on the structure, stability and kinetic behavior of Cr^{IV} species were obtained.

The rate reaction through which Cr^{IV} oxidizes substrates and its acidity dependence were both obtained in a few cases [41–43]. This work is the first to illustrate the kinetic behavior of Cr^{IV} with different neutral and acidic saccharides (Table 1) in order to determine their reactivity with Cr^{IV} and their possible contribution in genotoxicity.

* Corresponding author. Tel./fax: +54 341 4350214.
E-mail address: sala@iquir-conicet.gov.ar (L.F. Sala).

0277-5387/$ - see front matter © 2012 Elsevier Ltd. All rights reserved.
http://dx.doi.org/10.1016/j.poly.2012.09.042

Table 1
Bimolecular rate constants, k_4, for non acidic and acidic substrates. $[H^+] = 0.3$ M, I = 1.0 M, $T = 15$ °C. (**S1**) D-gluconic acid, (**P1**) 2-keto-D-gluconic acid; (**S2**) D-glucitol, (**P2**) D-gluconic acid; (**S3**) α-D-galactopyranose, (**P3**) D-galactonic acid; (**S4**) α-D-glucopyranose, (**P4**) D-gluconic acid; (**S5**) 2-desoxy-α-D-glucopyranose, (**P5**) 2-desoxy-D-gluconic acid; (**S6**) 6-desoxy-α-L-galactopyranose, (**P6**) 6-desoxy-α-L-galactonic acid; (**S7**) 3-*O*-methyl-α-D-glucopyranose, (**P7**) 3-*O*-methyl-D-gluconic acid; (**S8**) 1-methyl-α-D-galactopyranose, (**P8**) 1-methyl-α-D-galactofuranurono-6,3lactone; (**S9**) 1-methyl-α-D-glucopyranose, (**P9**) 1-methyl-α-D-glucofuranurono-6,3-lactone.

Substrate		Product		k (M^{-1} s^{-1})
S1	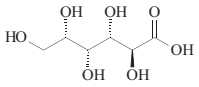	**P1**	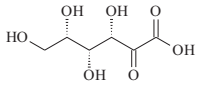	57 (6)
S2	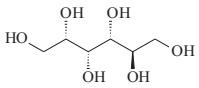	**P2**	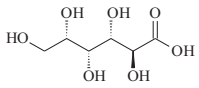	45 (5)
S3	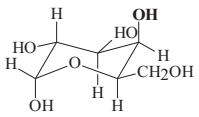	**P3**	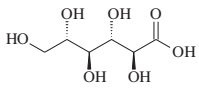	34 (4)
S4	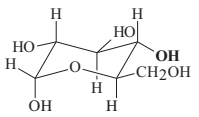	**P4**	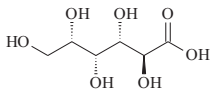	18 (2)
S5	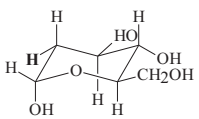	**P5**	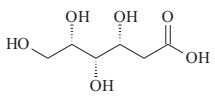	17 (2)
S6	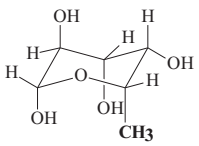	**P6**	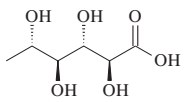	16 (2)
S7	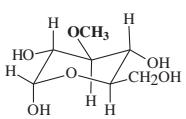	**P7**	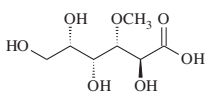	14 (1)
S8	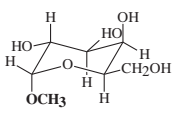	**P8**	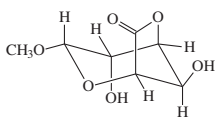	14 (1)
S9	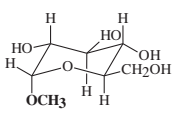	**P9**	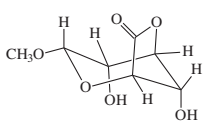	9 (1)

2. Experimental

2.1. Materials

D-Glucopyranose (Sigma 99.0%), 1-methyl-α-D-glucopyranose (Sigma 99.0%), 2-desoxi-D-glucopyranose (Sigma 99.0%), D-glucitol (Sigma 99.0%), 3-*O*-methyl-D-glucopyranose (Sigma 99.0%), D-galactopyranose (Sigma 99.0%), 1-methyl-α-D-galactopyranose (Sigma 99.0%), 6-desoxi-L-galactopyranose (Sigma 99.0%), D-gluconic acid sodium salt (Sigma, 99.0%), D-glucono-1,5-lactone (Sigma, 99.0%), 2-etil-2-hydroxibutiric acid, ehba (Sigma, 98%) sodium perchlorate monohydrate (Fluka 98.0%), oxygen (99.99%, Airliquid), perchloric acid (A.C.S. Baker), sodium hydroxide (Cicarelli, PA, ACS, ISO) Zn (Sigma–Aldrich, 99.0%), $HgCl_2$ (Cicarelli, PA, ACS, ISO), H_2SO_4 (Cicarelli, PA, ACS, ISO), $Cr(ClO_4)_3{\cdot}6H_2O$ (Sigma–Aldrich, 99.0%), D_2O (Sigma, 99.9% D). Aqueous solutions were prepared in milliQ water (18.0 MΩ/cm). $[Co^{III}(NH_3)_5Cl]Cl_2$ was synthesized according to the method described in the literature [44]. In experiments performed at constant ionic strength, I (1.0 M) and different hydrogen ion concentrations, mixtures of sodium perchlorate and perchloric acid solutions were used. The concentration of stock solutions of perchloric acid was determined by titration employing standard analytical methods.

Caution: Hg and Cr compounds are toxic and human carcinogens [45]. Contact with skin and inhalation must be avoided.

2.2. Methods

2.2.1. Substrate stability

The stability of the organic substrates with different experimental conditions as $HClO_4$ and oxygen concentrations – used in the kinetics measurements – were tested by High Performance Liquid Chromatography (HPLC). The chromatograms were obtained on a KNK-500A chromatograph provided with a 7125 HPLC pump. The effluent was monitored with refractive index (ERC-7522, ERMA INC) and UV (115 UV Gilson, λ 220 nm). The analysis was carried out on Aminex HPX-87H HPLC column (300 × 7.8 mm, Bio-Rad laboratories) using 3.2×10^{-2} M H_2SO_4 at 33 °C or an S5 amine resin Spherisorb HPLC column with a 73:27 mixture of acetonitrile (0.1 M) buffer phosphate at pH 6.4, as eluents. Organic saccharides were incubated during 1.0 h under the same experimental conditions used for the kinetics measurements. In all the cases, the chromatograms obtained from the incubated samples were identical to those without incubating.

2.2.2. Oxidation product analysis

The oxidation products of the aldoses/Cr^{IV} redox reaction were determined by HPLC. The chromatograms were obtained on a Varian Polaris 200 chromatograph provided with a cc Star 9000 HPLC pump. The separation was carried out on an anion-exchange Spherisorb S Sax HPLC column (250 × 4.6 mm) using 20 mM NaH_2PO_4 with 5% of ethanol as eluent and a flow rate of 0.5 mL min^{-1} at 44 °C. The effluent was monitored with a UV detector (Prostar 325 UV–Vis detector, λ = 210 nm). As an example, in the D-glucopyranose/Cr^{IV} system the $[H^+]$ of the reaction mixture samples was adjusted to 0.2 M by addition of $HClO_4$. All the samples were filtered through a 0.2 mm membrane prior to injection into the chromatographic system. Standard solutions of D-gluconic acid, D-glucono-1,5-lactone and D-glucopyranose were prepared individually in 0.20 M $HClO_4$ and the chromatographic R_t were determined separately. The mixture reaction of D-glucopyranose/Cr^{IV} shows two peaks with R_{t1} = 6.24 min and R_{t2} = 7.16 min. The acid media in the mixture reaction favored the lactonization process, and only the lactone peak was observed in the chromatogram (R_{t1}). The second peak (R_{t2}) refers to the remaining CrO_2^{2+} in the mixture reaction, as demonstrated with a standard of this compound, prepared with H_2O_2 and Cr^{VI} [46]. In addition, co-chromatography was performed, showing an increase of the D-glucono-1,5-lactone peak at 6.24 min.

2.2.3. Generation of Cr^{II}

Zn/Hg amalgam was prepared in a 50 mL balloon by stirring a mixture of Zn (10.0 g previously washed with 3.0 M HCl during 3.0 min) and $HgCl_2$ (0.3 M in 0.1 M HCl) for about 30 min. Afterwards, the excess of $HgCl_2$ was eliminated and the resulting amalgam washed three times with 1.0 M $HClO_4$ and finally with distilled water. An appropriate volume of $HClO_4$ and distilled water were added to the amalgam in the balloon, in order to reach pH 1.0 in a final volume of 35.0 mL. The balloon was then capped with a rubber septum and left with H_2 bubbling for, at least, 15 min to eliminate oxygen. After that, 1.0 mL of a 0.2 M $Cr(ClO_4)_3$ was injected and left to stir with H_2 bubbling. Three hours later, $Cr(ClO_4)_3$ was quantitatively reduced into Cr^{II}. The final $[Cr^{II}]$ was

determined by treating a reaction aliquot (0.5 mL Cr^{II}) with an aqueous solution of $[Co^{III}(NH_3)_5Cl]Cl_2$ (4.0 mL 2.1 mM) under anaerobic atmosphere (Ar). Then, 0.5 mL of this mixture was poured into a septum-capped spectrophotometric quartz cell, with a 1.0 cm path length, filled with 2.0 mL of concentrated HCl. The $[Co^{II}]$ was analyzed by measuring the absorbance of $[CoCl_4]^{2-}$ at 692 nm [44].

2.2.4. In situ generation of aqua oxo-Cr^{IV}, $(H_2O)_5$ CrO^{2+}

CrO^{2+} can be generated by rapid Cr^{II} oxygen-oxidation, according to the following procedure: a deoxygenated solution of Cr^{II} was injected into an acid aqueous solution of organic substrate saturated with oxygen (1.26 mM). In a typical experiment, 100 μL of 6.0 mM Cr^{II} were injected into a septum-capped spectrophotometric quartz cell, with a 1.0 cm path length, filled with 2.3 mL of an O_2-saturated solution containing appropriate concentrations of organic substrate, $HClO_4$ and $NaClO_4$ at 10–30 °C. At very low Cr^{II}/O_2 ratios (<0.05) superoxochromium^{III} (CrO_2^{2+}) is quantitatively formed, while at intermediate Cr^{II}/O_2 ratios (~0.15), the reaction affords mixtures of CrO^{2+}, Cr^{III} and CrO_2^{2+} [41,43]. Under these conditions, CrO^{2+} was immediately formed and reacted with the organic substrate to render Cr^{II} and oxidized organic products. This Cr^{II}, formed by the CrO^{2+}/organic substrate reaction is quantitatively transformed into CrO_2^{2+} (Cr^{II}/O_2 ratio <0.05) and no autocatalytic consumption of CrO_2^{2+} by Cr^{II} was observed [41,43].

2.2.5. Quantification of CrO^{2+}

The concentration of the generated CrO^{2+} species by the Cr^{II}/O_2 reaction at ~0.15 ratio can be easily determined by injection of 100 μL of 6.0 mM Cr^{II} into 2.3 mL of an O_2-saturated solution of 0.1 M ehba buffer at pH 3.0, 15 °C and I 1.0 M. Immediately after mixing, the solution turned pink and the absorbance of the mixture – due to $[Cr^{IV}(O)(ehba)_2]^{2-}$ – at 512 nm (ε = 2380 M^{-1} cm^{-1}) was measured [47]. The percentage of CrO^{2+} generated was calculated in two different ways. The first method employed was kinetic measurements at 512 nm of a mixture containing ehba buffer 0.1 M (pH 3.0), $[Cr^{II}]_0$ 0.3 mM and O_2 1.26 mM, at I 1.0 M and T 15 °C. In the second method, the Cr^{IV} was generated in the same experimental conditions without substrate. The Cr^{IV} was able to disproportion into Cr^{III} and Cr^{VI} and the reaction could be followed by the absorbance changes of the last species at 350 nm.

2.2.6. Characterization and stability of CrO_2^{2+}

One method used to characterize CrO_2^{2+} was a series of sequential spectra, between λ = 200 and 800 nm. This compound presents two intense characteristic absorption bands, at 290 nm (ε = 3100 M^{-1} cm^{-1}) and 245 nm (ε = 7000 M^{-1} cm^{-1}) with a relative intensity (Abs_{247}/Abs_{290}) of 2.2 [43]. A second method involved a specific reaction for CrO_2^{2+} [48] with Fe^{II}. Once the redox reaction Cr^{IV}/saccharide was finished, Fe^{II} was added to the mixture reaction (0.8 mM). Time evolution of the mixture was recorded every 2.0 min.

In order to study the influence of temperature, $[H^+]$ and I on CrO_2^{2+} stability, a series of experiments were carried out varying the parameters between 10 and 25 °C, 0.30 and 0.6 M and 0.2–1.0 M, respectively.

2.2.7. CrO^{2+}/saccharide kinetic measurements

All of the studied saccharides proved to be stable under kinetic experimental conditions. None of them, nor inorganic reagents or oxidation organic products absorbed at the wavelength chosen for the kinetic measurements. Kinetic measurements were monitored by absorbance changes on a Jasco V-530 spectrophotometer with fully thermostated cell compartments (±0.2 °C). Reactant solutions were thermostated prior to the experiment. The reactions were followed under pseudo-first-order conditions using excess of organic substrate over Cr^{IV}. The oxidation of different saccharides by CrO^{2+} was spectrophotometrically monitored following the appearance of CrO_2^{2+} as a final redox product at 290 nm [41]. All the saccharide/CrO^{2+} mixtures showed an increase in the bands at 290 and 245 nm, with relative intensity Abs_{247}/Abs_{290} = 2.2, characteristic of CrO_2^{2+} [41,43]. Mixtures containing substrate, $HClO_4$ and $NaClO_4$ did not show absorption at 290 nm, even after 10 min of oxygenation.

In all the kinetics measurements, $[Cr^{IV}]$, I, $[O_2]$, and temperature were kept constant at 0.07 mM, 1.0 M, 1.26 mM and 15–30 °C respectively. The concentration range of every organic substrate used was chosen in order to avoid CrO^{2+} disproportion. The proton dependence of the Cr^{IV}/saccharide reaction was studied varying $[HClO_4]$ between 0.3 and 0.6 M. For Cr^{IV}/D-galactopyranose and Cr^{IV}/D-glucopyranose mixtures the $[HClO_4]$ range was extended to 0.01–0.6 M. The kinetic isotope effect of the O–H hydrogen was studied performing the redox reaction in D_2O and comparing the results obtained with those in H_2O.

The experimental pseudo-first-order rate constants, k_{obs}, were obtained from nonlinear least square fits of absorbance data at 290 nm with averages of, as minimum, four determinations and within ±10% of each other. Data used to calculate the kinetic constant corresponded to 80% of the exponential growth of the absorbance experimental values. In every case, the first-order dependence of the rate upon $[Cr^{IV}]$ was verified in a set of experiments where the $[Cr^{IV}]_0$ was varied while T, [organic substrate], $[O_2]$ and I were kept constant.

3. Results and discussion

Under anaerobic conditions, Cr^{II} reduces Co^{III} complex into Co^{II} according Eq. (1):

$$[Co(NH_3)_5Cl]Cl_2 + Cr^{2+} + 6HCl \rightarrow CoCl_4^{2-} + 5H_4NCl + Cr^{3+} + H^+ \quad (1)$$

The observed spectrum was in agreement with those reported for $CoCl_4^{2-}$ in the literature [41]. The content of Cr^{IV} was determined (see experimental section) as $[Cr^{IV}(O)(ehba)_2]$.

Under the experimental conditions above mentioned, reaction between Cr^{II} and O_2 rapidly produced 0.07 mM CrO^{2+} (29.6% average based on total $[Cr^{II}]$) (See Supplementary Materials Figures S1a and S1b).

Cr^{IV} is an unstable species [41,43] with a 0.75 min-half life at 0.1 M ionic strength in acid media and room temperature [43]. This chromium species can participate in two different and competitive reactions: organic substrates oxidation and disproportion into Cr^{VI} and Cr^{III} through Cr^{V}, according to Eqs. (2)–(4):

$$2Cr^{IV} \rightarrow Cr^{III} + Cr^{V} \quad (2)$$

$$Cr^{V} + Cr^{IV} \rightarrow Cr^{VI} + Cr^{III} \quad (3)$$

$$3Cr^{IV} \rightarrow Cr^{VI} + 2Cr^{III} \quad (4)$$

Since Cr^{VI} also absorbs at 290 nm, where kinetics measurements are studied, it is important to verify that disproportion process does not occur. For this reason, it is necessary to determine the specific experimental conditions where substrates oxidation reactions are favored over disproportion. Fig. 1 shows a comparison between the corresponding spectra for CrO_2^{2+} and Cr^{VI}. As can be seen, there is a region where both spectra are superimposed (230–330 nm), but absorbance at 350 nm is only due to Cr^{VI}. Therefore disproportion, if any, can be observed at 350 nm because of Cr^{VI} formation. With the purpose of avoiding Cr^{VI} generation via disproportion, a minimum concentration of saccharide is required. Such minimum concentration depends on the Cr^{IV}/saccharide redox reaction rate and is determined for each organic substrate.

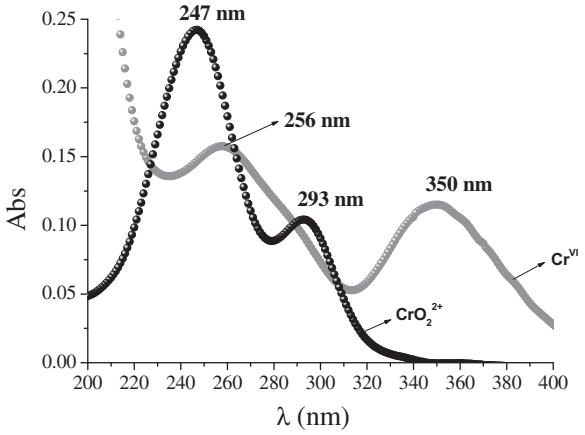

Fig. 1. Comparison between CrO_2^{2+} and Cr^{VI} spectra. $[CrO_2^{2+}]$ = 0.032 mM (black); $[Cr^{VI}]$ = 0.08 mM (gray); $[O_2]$ = 1.26 mM; $[H^+]$ = 0.3 M; I = 1.0 M; T = 15 °C.

The other possible Cr^{VI} generation, which is the bimolecular decomposition of CrO_2^{2+} (Eq. (5)), do not occur [49] as stated in Section 2:

$$2CrO_2^{2+} + 4H_2O \rightarrow 2\ HCrO_4^- + 6H^+ \quad (5)$$

Experimental results show that Cr^{IV} disproportion is always negligible comparable to its capacity to oxidize the organic substrate. Only in absence or very low concentration of substrate, an important increment of absorbance at 350 nm can be observed due to the increase in the Cr^{VI} formation (data not shown). Total Cr^{IV} disproportion occurring in the absence of substrate (Eqs. (2)–(4)) can be used to quantify this species. According to Eq. (4), initial concentration of Cr^{IV} was calculated from the absorbance at 350 nm. The resulting value was 0.0705 mM, which represents 28% of total chromium, in agreement with the $[Cr^{IV}(O)(ehba)_2]$ formation at pH 3.0.

3.1. CrO_2^{2+} determination and characterization

For every CrO^{2+}/substrate reaction, the CrO_2^{2+} formed was identified by analyzing its sequential electronic spectra, where its characteristic absorption bands were observed, in agreement with literature [41,43] data. The ratio Abs_{290}/Abs_{245} remains constant in time when CrO_2^{2+} slowly decomposes to Cr^{III} species (See Supplementary Materials Fig. S2).

Additionally, the presence of CrO_2^{2+} was verified by means of their well-known reaction with Fe^{II} (Eq. (6)):

$$CrO_2^{2+} + 3Fe^{2+} + 4H^+ \rightarrow Cr^{3+} + 3Fe^{3+} + 2H_2O \quad (6)$$

Every spectrum recorded was subtracted from the CrO_2^{2+} spectrum, prior to the Fe^{II} addition. After the correction of the small dilution, a negative absorbance around 290 nm was obtained confirming the presence of CrO_2^{2+} [49] (See Supplementary Materials Fig. S3).

3.2. Influence of temperature, $[H^+]$ and I on CrO_2^{2+} stability

The CrO_2^{2+} produced in the CrO^{2+}/saccharide mixtures slowly decomposes into Cr^{III} species. However, in the time scale of kinetic measurements, CrO_2^{2+} is stable enough to be considered as the final product of the redox reaction. The rate of CrO_2^{2+} decay is faster at higher temperatures. That means the stability of CrO_2^{2+} diminishes with temperature increment. When two different $[H^+]$ were used to perform the same reaction at constant temperature and ionic strength, there were no changes in the rate decay of CrO_2^{2+}. This implies that $[H^+]$ does not alter its stability during the redox reaction time (See Supplementary Materials Fig. S4). Finally, at constant $[H^+]$ and temperature, two different values of ionic strength (0.2 and 1.0) were studied. Kinetic profiles show that the rate decay of CrO_2^{2+} is not affected significantly, even using values five times higher of ionic strength, in the kinetics times of the measurements (data not shown).

It must be highlighted that the effect of substrate concentration was studied to verify any possible reaction between the CrO_2^{2+} and saccharides present in the mixture, which would affect CrO_2^{2+} stability. The CrO_2^{2+} decay rate remained unaffected regardless of the substrate concentration used (see Supplementary Materials Fig. S5). An independent prepared solution of CrO_2^{2+} decays at the same rate as CrO_2^{2+} formed in the saccharide/Cr^{IV} reactions if experimental conditions are the same [50].

According to the mentioned above, kinetic conditions should be accurately selected in order to guarantee that: (a) CrO^{2+} disproportion reaction should be negligible respect to its capacity to oxidize the organic substrate; (b) CrO_2^{2+} should be stable enough to be considered as the final redox product of the CrO^{2+}/saccharide reaction and (c) oxidation rate should be slow enough to be measured in a conventional spectrophotometer.

3.3. Kinetic measurements: saccharide/Cr^{IV} reactions

As mentioned before, CrO^{2+} is a relatively unstable species [41,43]. With the purpose of studying CrO^{2+} oxidation process over different organic substrates, it was generated in situ as described in the experimental section. The CrO^{2+} generated reacts with the substrate present in the reaction media to give Cr^{II} and oxidized organic substrate (Eq. (7)). The newly generated Cr^{II} is efficiently trapped by oxygen in a fast reaction ($k = 1.6 \times 10^8$ [51]) to quantitatively produce CrO_2^{2+} (Eq. (8)) [41,43,49]. This reaction has been extensively studied by pulse radiolysis [52], UV spectrophotometry [46] and Raman spectroscopy [53]. The CrO_2^{2+} generated in this reaction slowly decomposes into Cr^{III} (Eq. (9)):

$$Cr^{IV} + S \rightarrow Cr^{II} + S_{ox}\ (\text{slow}) \quad (7)$$

$$Cr^{II} + O_2 \rightarrow CrO_2^{2+}\ (\text{fast}) \quad (8)$$

$$CrO_2^{2+} \rightarrow\rightarrow\rightarrow\rightarrow Cr^{III}\ (\text{very slow}) \quad (9)$$

The CrO_2^{2+} species is selected as a final product redox in order to follow the CrO^{2+}/saccharides kinetics because: (a) it has a defined and characteristic spectrum in aqueous solution [41,43] and (b) it is stable in the kinetics times. This species rapidly comes from the Cr^{II} formed (Eqs. (7) and (8)) and slowly decomposes into Cr^{III} species, Fig. 2a and Eq. (9); (c) no species present in the reaction media, except for CrO_2^{2+}, absorb at 290 nm and (d) no saccharide/CrO_2^{2+} reaction was observed.

Although CrO^{2+} generated in situ has a characteristic spectrum, all the other species (CrO_2^{2+} and Cr^{III}) have superimposed spectra, making it impossible to determine the individual contribution of every species to the absorbance at 290 nm. For this reason, the redox process is followed by CrO_2^{2+} formation instead of CrO^{2+} disappearance.

Moreover, the route of CrO^{2+} disproportion (Eqs. (2)–(4)) and the bimolecular decomposition (Eq. (5)) are not favored under the experimental conditions used in this work. These facts ensure that the increase of the absorbance at 290 nm – due to generation of CrO_2^{2+} (Eq. (8)) – is a direct reflection of the CrO^{2+}decrease when reacting with organic substrate.

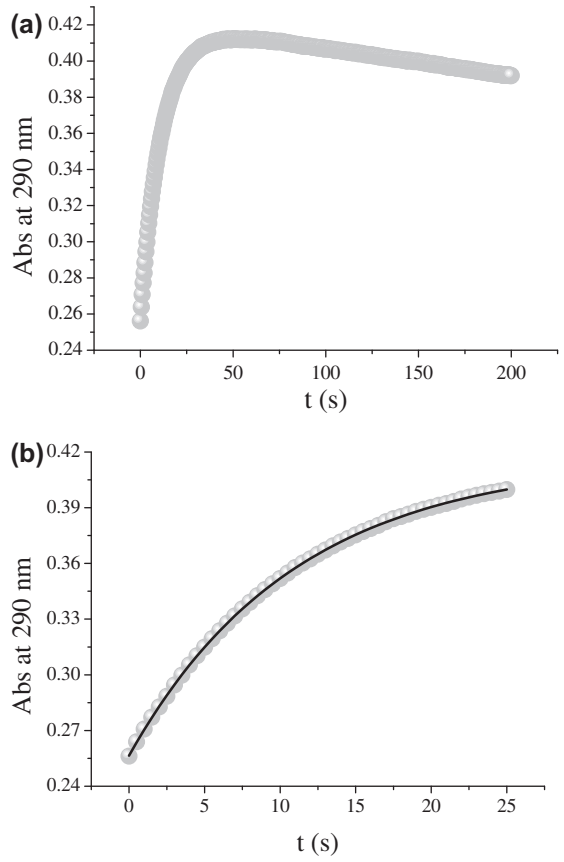

Fig. 2. (a) Kinetic profile of saccharide oxidation, Abs_{290} vs. time. [D-Glucopyranose] = 5.0 mM; $[H^+]$ = 0.3 M; $[CrO^{2+}] \sim 0.07$ mM; $[O_2]$ = 1.26 mM; T = 15 °C; I = 1.0 M; λ = 290 nm. (b) Mathematical fitting of the experimental kinetic data; k_{obs} was obtained using Eq. (10).

3.4. Determination of the oxidation rate, k_{obs}

The kinetic data oxidation of different saccharides by CrO^{2+} was spectrophotometrically monitored following the appearance of $CrO_2{}^{2+}$ as a final redox product at 290 nm and 15 °C. These data were set in an Abs_{290} versus time graphic, producing for all substrates/CrO^{2+} mixtures, curves with a biphasic behavior, Fig. 2a. The first part of the graphic exhibits a rapid exponential increment and corresponds to the $CrO_2{}^{2+}$ formation (Eqs. (7) and (8)); while the slower second part corresponds to $CrO_2{}^{2+}$ decay into Cr^{III} species (Eq. (9)). The experimental kinetic constants, k_{obs}, were calculated using a non-linear least square fits of 80% of the experimental data exponential growth, according to Eq. (10), Fig. 2b:

$$Abs = Abs_{inf} + (Abs_0 - Abs_{inf})e^{(-k_{obs}\cdot t)} \quad (10)$$

where Abs_0, Abs_{inf} and Abs represent respectively absorbance at zero, infinite and t time and k_{obs} is the rate constant for substrate oxidation by CrO^{2+}.

The effect of [substrate] on k_{obs} for non-acidic substrates is shown in Fig. 3. As represented in the graphic, a family of straight lines with zero intercept is obtained; the slopes of these lines represent the bimolecular rates constants summarized in Table 1. No dependence of the rate constant, $k_{obs,}$ with $[H^+]$ was observed. The experimental rate law for these reactions can be expressed as shown in Eq. (11):

$$-d[Cr^{IV}]/dt = d[CrO_2{}^{2+}]/dt = k_4[substrate][CrO^{2+}] \quad (11)$$

As illustrated in Table 1 and Fig. 3, the reactivity order for non-acidic substrates is the following: 1-methyl-α-D-glucopyranose << 1-methyl-α-D-galactopyranose ~ 3-*O*-methyl-D-glucopyranose ~ 6-desoxi-L-galactopyranose ~ 2-desoxi-D-glucopyranose ~ D-glucopyranose << D-galactopyranose << D-glucitol. Taking into account the corresponding structure of each substrate (Table 1), we notice that open chain saccharide, D-glucitol, reacts much faster than those with a cyclic structure. From the experimental results various observations can be made: (a) D-galactopyranose oxidation rate is almost twice higher than D-glucopyranose, indicating that a change in the orientation of the hydroxyl group in C4, Table 1, clearly modifies the saccharide reactivity towards CrO^{2+}; (b) the absence of hydroxyl group in C2 (2-desoxi-D-glucopyranose) does not affect the rate constant; (c) the methylation on C3 (3-*O*-methyl-D-glucopyranose) does not affect significantly the rate constant and (d) saccharides methylated in C1 (1-methyl-α-D-glucopyranose and 1-methyl-α-D-galactopyranose) are notoriously less reactive than the corresponding aldopyranoses. In the knowledge that the CrO^{2+}/saccharides redox reactions yield aldonic acids, it can be postulated that the most reactive site in aldopyranoses is C1.

The tendency observed in the redox reactivity of the saccharides towards CrO^{2+} can be rationalized by considering the relative instability of the saccharide-CrO^{2+} chelate formed before the redox reactions. The highest reactivity of D-galactopyranose with CrO^{2+} can be a consequence of saccharide-CrO^{2+} complex instability induced by the non-bound 1,3-diaxial interactions [18,23]. Thus, the O^4a:H^2a steric interaction in the D-galactopyranoside stereoisomer should have the highest rate accelerating effect, Scheme 1. By the contrary, D-glucopyranose with all the ring substituents in pseudoequatorial position forms the most thermodynamically stable complex and is oxidized more slowly than D-galactopyranose, as observed. The elimination of the equatorial hydroxyl group in C2 (2-desoxi-D-glucopyranose) and the methylation of an OH in C3 (3-*O*-methyl-D-glucopyranose) do not essentially modify the rate of these saccharides oxidation by CrO^{2+}. A possible explanation for such behavior is that the modified OH belongs to the axial type. Because of this reason, there are not changes in the rings stability. This way, the saccharides, D-glucopyranose, 2-desoxi-D-glucopyranose and 3-*O*-methyl-D-glucopyranose are oxidized by CrO^{2+} practically at the same rate (see Scheme 2).

Regarding the 6-desoxi-L-galactopyranose, Scheme 1, there are two types of 1,3-diaxial interactions, as a result, this saccharide should react faster than D-galactopyranose. The obtained results cannot be explained in term of tensional effects. For this reason, there might be additional stabilization factors in the CrO^{2+}-6-desoxi-L-galactopyranose complex which justify this saccharide low reactivity (Table 1). A suitable explanation would probably be a different conformation of the aldose in the intermediate complex. The same behavior has been observed in the 6-desoxi-L-galactopyranose oxidation by Cr^{VI} [23].

Finally, in aqueous solution, saccharides are in fast equilibrium between their cyclic and open form. However, the low concentration of the open form [54] present in D-galacto and D-glucopyranose solutions and the high reactivity of the α(β)-1-methyl-galactopyranose respect to α(β)-1-methyl-glucopyranose with Cr^{VI} indicate that the saccharide reactive form is the cyclic one [18].

The activation parameters, Table 2, for CrO^{2+}/D-galactopyranose and CrO^{2+}/D-glucopyranose reactions were calculated from the plot of $\ln(k/T)$ versus $1/T$, Fig. 4.

The isokinetic relationship plot, Fig. 5, shows that $\Delta H^{\ddagger}$ is a linear function of $\Delta S^{\ddagger}$ for the reactions of primary, secondary alcohols, 1,2-cyclohexanediols and saccharides with CrO^{2+}. The existence of an isokinetic relationship supports that a single mechanism operates along the series of compounds. Certain members deviating from the correlation to a significant extent suggests that a

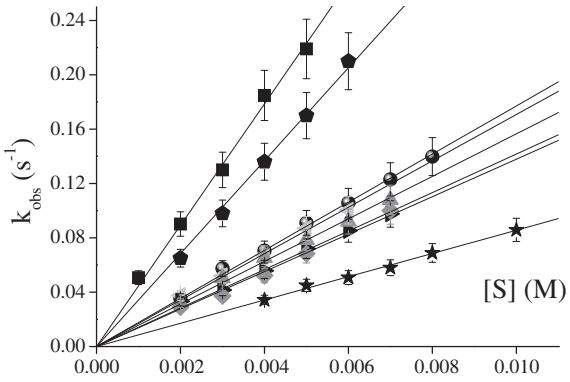

Fig. 3. Effect of [substrate] on k_{obs}. $[CrO^{2+}] \sim 0.07$ mM; $T = 15$ °C, I = 1.0 M; $[H^+] = 0.3$ M; $[O_2] = 1.26$ mM.

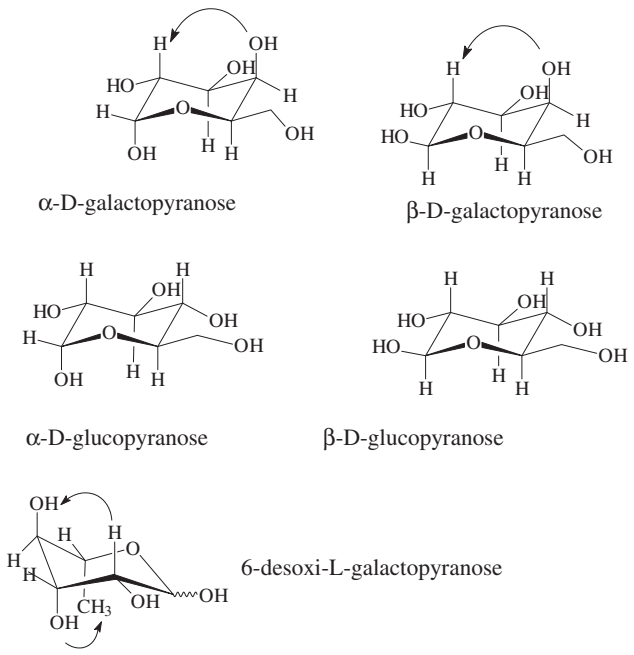

Scheme 1. Non-bound 1,3-diaxial interactions.

different mechanism takes place. This deviation occurs with the activation parameters derived from phenol/CrO^{2+} reaction [55].

The oxidation mechanism by CrO^{2+} of the linear and cyclic alcohols mentioned above has been accurately demonstrated by Espenson and coworkers [41,50] as a hydride transfer from the saccharide to the CrO^{2+}. Fig. 5 clearly depicts the existence of an isokinetic relationship and consequently makes it possible to postulate the same mechanism for the saccharide oxidation by CrO^{2+}. The slope of Fig. 5 represents the isokinetic temperature, whose value is 336 K (63 °C), in agreement with the one obtained from Fig. 4.

The kinetic isotope effect of the O–H hydrogens was negligible ($k_H/k_D = 1.2$) for D-glucopyranose/CrO^{2+} redox reaction. Both this result and the formation of Cr^{II} as a redox product suggest that the saccharides oxidation takes place by a concerted two-electron hydride transfer mechanism [50]. Hydride transfer is generally characterized by a positive value of ΔH and large negative values of ΔS. The latter have been attributed to the strict orientation requirements for hydride and achievement of the cyclic transition value of ΔS. In case that organic radical and Cr^{III} are products of the redox reaction, Cr^{III} must be reduced to Cr^{II} by the organic radical. Reaction between Cr^{II} and oxygen generate CrO_2^{2+}, which is thermodynamically possible (E^0 $Cr^{III}/Cr^{II} = -0.416$ V), has been shown not to occur because is too slow ($k = 5.6 \times 10^2$ L mol^{-1} s^{-1} [56]). Therefore, the only way to obtain Cr^{II} (and CrO_2^{2+}) in the saccharide/Cr^{IV} oxygenated mixtures is by a two-electron reduction of Cr^{IV} species.

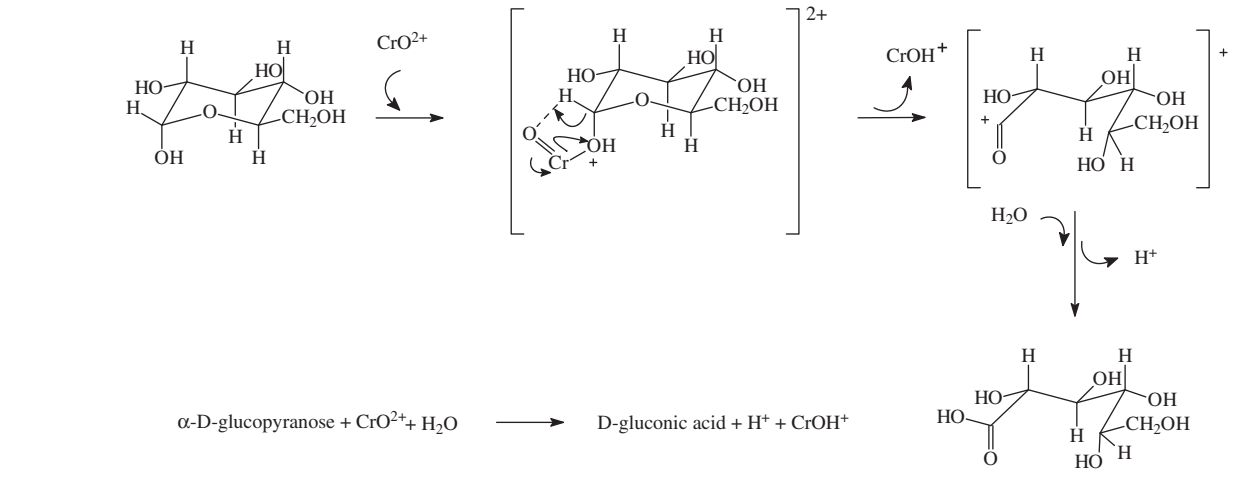

Scheme 2. Proposed mechanism for the oxidation of glucose.

Table 2
Activation parameters for the CrO_2^{2+} oxidation of D-glucopyranose, D-galactopyranose, diols, methanol, 2-propanol and cyclobutanol.

Substrate	Activation parameters		
	$\Delta H^{\ddagger}$ (kJ mol^{-1})	$\Delta S^{\ddagger}$ (J mol^{-1} K^{-1})	Ref.
D-Glucopyranose	34	−100	This work
D-Galactopyranose	44	−68	This work
cis-1,2-Cyclohexanediol	41	−78	[50]
trans-1,2-Cyclohexanediol	51	−48	[50]
Methanol	34	−98	[41]
2-Propanol	33	−112	[41]
Cyclobutanol	46	−61	[41]

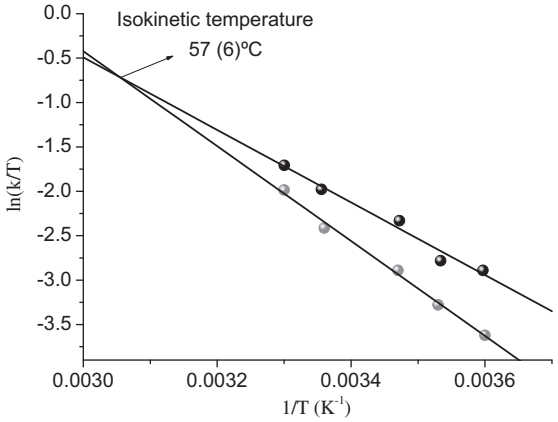

Fig. 4. Plot of $\ln(k/T)$ vs. T^{-1} for the reaction of D-galactopyranose and D-glucopyranose with CrO^{2+}. [Substrate] = 1.0 mM; I = 1.0 M; [Cr^{IV}] ~ 0.07 mM; [O_2] = 1.26 mM; T = 10–25 °C; [H^+] = 0.30 M.

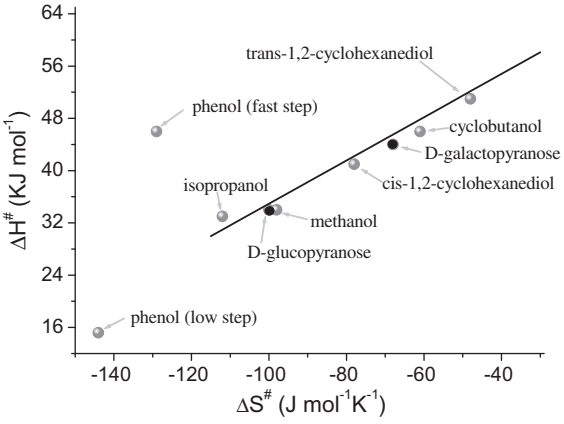

Fig. 5. Plot of $\Delta H^{\ddagger}$ vs. $\Delta S^{\ddagger}$ for the reactions of primary, secondary alcohols, 1,2-cyclohexanediols and saccharides with CrO^{2+}.

As previously commented, oxidation of aldopyranose by Cr^{IV} was independent of [H^+]. Concerning the case of the D-gluco and D-galactopyranose/Cr^{IV} reaction, the experimental rate low was valid at pH 2. This pH can be found in subcellular compartments like phagosomes [57].

Formation of Cr^{V} and/or Cr^{IV} intermediates in the redox reaction with Cr^{VI} has been previously observed for the chromic oxidation of organic substrates [58]. For all oxidation reactions of these substrates with Cr^{VI}, the presence of Cr^{IV} has been demonstrated, but only in few cases the rate constants of Cr^{IV}/substrate were

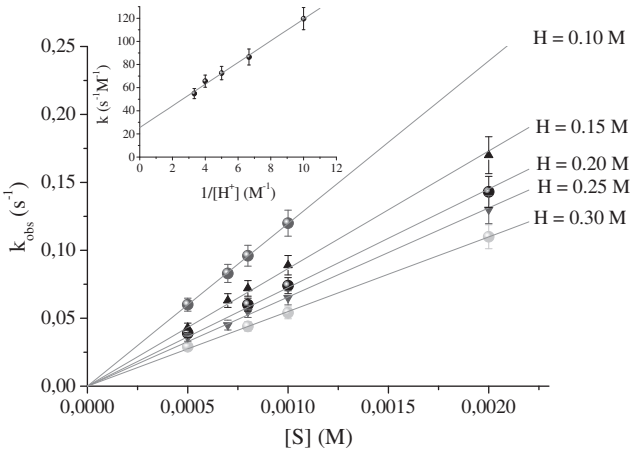

Fig. 6. Effect of [D-gluconic acid] on k_{obs}. Insert: D-gluconic acid rate constant, k_4, dependence with [H^+]. [Cr^{IV}] ~ 0.07 mM; T = 15 °C, I = 1.0 M; [O_2] = 1.26 mM.

determined [28–30,59]. The obtained result in this work confirms that Cr^{IV} is a more reactive species towards saccharides than Cr^{VI} or Cr^{V}. In fact the oxidation rate values for the Cr^{IV}/saccharide are, at least, two orders of magnitude higher than the oxidation rates for Cr^{V}/saccharide or Cr^{VI}/saccharide reactions.

On the other hand, as demonstrated in previous works [29,59], acidic substrates like D-galacturonic and D-glucuronic acid, have a completely different behavior when reacting with Cr^{IV}. The experimental rate law of saccharide/Cr^{IV} reaction obtained for these substrates exhibits a strong inhibition of the redox process when [H^+] increases. Experimental results from D-gluconic acid shows the same behavior, as can be seen in Fig. 6. As represented in Fig. 6, plots of k_{obs} versus [D-gluconic acid] gave good straight lines from which slope k_{4H} values were determined (Eq. (12)). The bimolecular rate constant, k_{4H}, varied linearly with $[H^+]^{-1}$ with a positive intercept $k_a = 25.5 \pm 2.4\ s^{-1}\ M^{-1}$ and slope $k_b = 9.4 \pm 0.4\ s^{-1}$, Eq. (13) and Fig. 6:

$$K_4 = k_{4H}[\text{D-gluconic}] \quad (12)$$

$$K_{4H} = k_a + k_b[H^+]^{-1} \quad (13)$$

The rate constant for Cr^{IV} disappearance is given by Eq. (14):

$$K_4 = (k_a + k_b[H^+]^{-1})[\text{D-gluconic acid}] \quad (14)$$

The bimolecular rate constant was inversely proportional with [H^+] in the range 0.1–0.3 M. The rate law was resolved using the already known acid–base equilibrium between the carboxylic acid, HS-COOH, and the conjugate base, HS-COO^-, Scheme 3.

Scheme 3 shows that two species are able to react with CrO^{2+} in parallel slow steps to give Cr^{II} and oxidized organic product (P). In this scheme, k_1 and k_2 represent the rate constants for the oxidation of the D-gluconic acid (HS-COOH) and the conjugate base (HS-COO^-) respectively, which leads to Eq. (15):

$$K_4 = k_1[\text{HS-COOH}] + k_2[\text{HS-COO}^-] \quad (15)$$

Taking into account that:

$$K_a = \frac{[H^+][\text{HS-COO}^-]}{[\text{HS-COOH}]}$$

and

$$[\text{HS-COOH}]_T = [\text{HS-COOH}] + [\text{HS-COO}^-]$$

and making the corresponding mathematical arrangements, Eq. (15) transforms into Eq. (16)

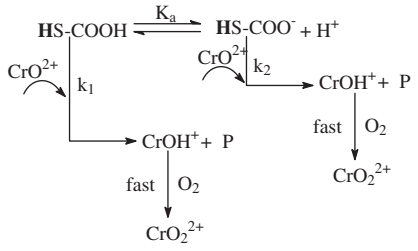

Scheme 3. Proposed mechanism of CrO^{2+} reaction with D-gluconic acid.

$$k_4 = \left[\frac{[H^+]k_1 + k_2K_a}{[H^+] + K_a}\right][\text{HS-COOH}]_T \quad (16)$$

since $[H^+] >> Ka$ [60], thus

$$k_4 = \left[\frac{[H^+]k_1 + k_2K_a}{[H^+]}\right][\text{HS-COOH}]_T = (k_1 + k_2K_a[H^+]^{-1})[\text{HS-COOH}]_T \quad (17)$$

$$-d[Cr^{IV}]/dt = d[CrO_2{}^{2+}]/dt = (k_1 + k_2K_a[H^+]^{-1})[\text{HS-COOH}]_T[CrO^{2+}] \quad (18)$$

The rate law for the disappearance of Cr^{IV} takes the form of Eq. (18), which is in total agreement with the experimental rate law, Eq. (14) where $k_1 = k_a$ and $k_2K_a = k_b$.

The k_b rate constant is larger than the rate constant for oxidation of HS-COOH in the 0.1–0.3 M range of $[H^+]$, possibly due to the formation of the precursor complex from oppositely charged ions.

This happens to be the same expression used in previous works, corroborating that the oxidation rate of acidic saccharides by CrO^{2+} is strongly inhibited when $[H^+]$ increases.

4. Conclusions

In this paper we studied the oxidation reactions kinetics of a series of related saccharides by aqua-oxo chromium(IV), in perchloric acid aqueous solutions. These reactions yield superoxochromium(III) ion, $CrO_2{}^{2+}$, providing evidence that the two-electron reduction of CrO^{2+} to Cr^{2+} occurred in a single step. Relative reactivities of these saccharides towards CrO^{2+} reduction are: 1-methyl-α-D-glucopyranose << 1-methyl-α-D-galactopyranose ~ 3-*O*-methyl-D-glucopyranose ~ 6-desoxi-L-galactopyranose ~ 2-desoxi-D-glucopyranose ~ D-glucopyranose << D-galactopyranose << D-glucitol. The CrO^{2+}/saccharides redox reactions yield aldonic acids as products, evidencing that the most reactive site in aldopyranoses is C1.

The oxidation of aldonic acid such as D-gluconic acid by CrO^{2+} showed the same mechanisms but the redox process is strongly inhibited when $[H^+]$ increases. On the basis of kinetics, activation parameters and product data, the mechanism of saccharides oxidation by CrO^{2+} was proposed to be a direct hydride-ion transfer.

Acknowledgments

Luis F. Sala acknowledges the Nacional Research Council of Argentina (CONICET), Nacional University at Rosario (UNR) and the Santa Fe Province Programs of Promotion for the Scientific and Technological Activities for financial support.

Appendix A. Supplementary data

Supplementary data associated with this article can be found, in the online version, at http://dx.doi.org/10.1016/j.poly.2012.09.042.

References

[1] International Agency for Research on Cancer (IARC). Overall Evaluations of Carcinogenicity to Humans, IARC, 203. Available from: <http://www.iarc.fr>.
[2] J. Guertin, J.A. Jacobs, C.P. Avakian (Eds.), Chromium (VI) Handbook, CRC Press, Boca Raton, 2005.
[3] R. Codd, J.A. Irwin, P.A. Lay, Curr. Opin. Chem. Biol. 7 (2003) 213.
[4] A. Levina, L. Zhang, P.A. Lay, J. Am. Chem. Soc. 132 (2010) 8720.
[5] G. Barr-David, T. Hambley, J.A. Irwin, R. Judd, P.A. Lay, B.D. Martin, R. Bramley, N.E. Dixon, P. Hendry, J. Ji, R. Baker, A. Bonin, Inorg. Chem. 31 (1992) 4906.
[6] K.D. Sugden, K.E. Wetterhahn, J. Am. Chem. Soc. 118 (1996) 10811.
[7] D.M. Stearns, K.E. Wetterhahn, Chem. Res. Toxicol. 10 (1997) 271.
[8] A. Levina, R. Codd, P.A. Lay, in: G.R. Hanson, L.J. Berliner (Eds.), Biological Magnetic Resonance, vol. 28, Part 4, Springer, New York, 2009, pp. 551–579.
[9] K.D. Sudgen, D.M. Stearns, J. Environ. Pathol. Toxicol. Oncol. 19 (2000) 215.
[10] R. Codd, C.T. Dillon, A. Levina, P.A. Lay, Coord. Chem. Rev. 216–217 (2001) 537.
[11] S. Signorella, C. Palopoli, M. Santoro, S. García, V. Daier, J.C. González, V. Roldán, M.I. Frascaroli, M. Rizzotto, L.F. Sala, Trends Inorg. Chem. 7 (2001) 197.
[12] B. Gyurcsik, L. Nagy, Coord. Chem. Rev. 203 (2000) 81.
[13] A. Levina, R. Codd, C.T. Dillon, P.A. Lay, Prog. Inorg. Chem. 51 (2003) 145.
[14] A.K. Das, Coord. Chem. Rev. 248 (2004) 81.
[15] A. Levina, P.A. Lay, Coord. Chem. Rev. 249 (2005) 281.
[16] M. Stefanikou, C. Maravelias, Curr. Top. Toxicol. 1 (2004) 161.
[17] G.N. Babu, R. Ranjani, G. Farceda, S.D.S. Murthy, J. Phytol. Res. 20 (2007) 1.
[18] M. Rizzotto, A. Levina, M. Santoro, S. García, M.I. Frascaroli, S. Signorella, L.F. Sala, P.A. Lay, J. Chem. Soc., Dalton Trans. (2002) 3206.
[19] V. Roldán, J.C. González, M. Santoro, S. García, N. Casado, S. Olivera, J.C. Boggio, J.M. Salas-Peregrin, S. Signorella, L.F. Sala, Can. J. Chem. 80 (2002) 1676.
[20] S. Signorella, R. Lafarga, V. Daier, L.F. Sala, Carbohydr. Res. 324 (2000) 127.
[21] S. Signorella, M.I. Frascaroli, S. García, M. Santoro, J.C. González, C. Palopoli, V. Daier, N. Casado, L.F. Sala, J. Chem. Soc., Dalton Trans. (2000) 1617.
[22] M. Rizzotto, V. Moreno, S. Signorella, V. Daier, L.F. Sala, Polyhedron 19 (2000) 417.
[23] S. Signorella, V. Daier, S. García, R. Cargnello, J.C. González, M. Rizzotto, L.F. Sala, Carbohydr. Res. 316 (1999) 14.
[24] S. Signorella, S. García, L.F. Sala, J. Chem. Educ. 76 (1999) 405.
[25] M.I. Frascaroli, J.M. Salas-Peregrin, L.F. Sala, S. Signorella, Polyhedron 28 (2009) 1049.
[26] L.F. Sala, J.C. Gonzalez, S.I. García, M.I. Frascaroli, S. Van Doorslaer, in: D. Horton (Ed.), Advances in Carbohydrate Chemistry and Biochemistry, first ed., vol. 66, Elsevier, Amsterdam, 2011, pp. 69–120.
[27] J.C. González, S.I. García, S. Bellú, A.M. Atria, J.M. Salas Peregrin, A. Rockenbauer, L. Korecz, S. Signorella, L.F. Sala, Polyhedron 28 (2009) 2719.
[28] S.E. Bellú, J.C. González, S.I. García, S. Signorella, L.F. Sala, J. Phys. Org. Chem. 21 (2008) 1059.
[29] M.F. Mangiameli, J.C. González, S. García, S. Bellú, M. Santoro, E. Caffaratti, M.I. Frascaroli, J.M. Salas Peregrín, A.M. Atria, L.F. Sala, J. Phys. Org. Chem. 23 (2010) 960.
[30] M.F. Mangiameli, J.C. González, S.I. García, M.I. Frascaroli, S. Van Doorslaer, J.M. Salas Peregrin, L.F. Sala, Dalton Trans. 40 (2011) 7033.
[31] A. Levina, R. Codd, C.T. Dillon, P. Lay, Prog. Inorg. Chem. 51 (2002) 145.
[32] C.T. Dillon, Ph.D. Thesis, University of Sydney, 1995.
[33] K.J. Liu, X. Shi, J. Jiang, F. Goda, N. Dalal, H.M. Swartz, Ann. Clin. Lab. Sci. 26 (1996) 176.
[34] A. Levina, R. Codd, C.T. Dillon, P. Lay, Prog. Inorg. Chem. 51 (2006) 145.
[35] L.F. Larkworthy, K.B. Nolan, P. O'Brien, in: G. Wilkinson, R.D. Gillard, J.A. McCleverty (Eds.), Comprehensive Coordination Chemistry, vol. 3, Pergamon Press, Oxford, UK, 1987, pp. 699–969.
[36] P. Lay, A. Levina, Coord. Chem. Rev. 249 (2005) 281.
[37] L.F. Sala, J.C. González, S. García, M.I. Frascaroli, M.F. Mangiameli, Global J. Inorg. Chem. 2 (2010) 18.
[38] R. Codd, P.A. Lay, A. Levina, Inorg. Chem. 36 (1997) 5440.
[39] R.P. Farrell, R.J. Judd, P.A. Lay, N.E. Dixon, R.S. Baker, A.M. Bonin, Chem. Res. Toxicol. 2 (1989) 227.
[40] C.T. Dillon, P.A. Lay, A.M. Bonin, N.E. Dixon, T.J. Collins, K.L. Kostka, Carcinogenesis 14 (1993) 1875.
[41] S.L. Scott, A. Bakac, J.H. Espenson, J. Am. Chem. Soc. 114 (1992) 4205.
[42] A. Bakac, J.H. Espenson, Acc. Chem. Res. 26 (1993) 519.
[43] S. Scott, A. Bacak, J. Espenson, J. Am. Chem. Soc. 113 (1991) 7787.
[44] O.A. Babich, E.S. Gould, Inorg. Chem. 40 (2001) 5708.
[45] International Agency for Research on Cancer: chromium, nickel and welding, in: IARC Monographs on the Evaluation of the Carcinogenic Risk of Chemicals for Humans, Lyon, France, 1990.
[46] A. Bakac, S.L. Scott, J.H. Espenson, K.R. Rodgers, J. Am. Chem. Soc. 117 (1995) 6483.
[47] R. Codd, P. Lay, A. Levina, Inorg. Chem. 36 (1997) 5440.
[48] O. Petovsky, A. Bacak, J.H. Espenson, J. Am. Chem. Soc. 120 (1998) 13422.
[49] M.E. Brynildson, A. Bakac, J.H. Espenson, J. Am. Chem. Soc. 109 (1987) 4579.
[50] A. Al-Ajlouni, A. Bakac, J.H. Espenson, Inorg. Chem. 33 (1994) 1011.
[51] Y.A. Ilan, G. Czapski, M. Ardon, Isr. J. Chem. 13 (1975) 15.
[52] R.M. Sellers, M.G. Simic, J. Am. Chem. Soc. 98 (1976) 4579.
[53] A. Bakac, T. Won, J.H. Espenson, Inorg. Chem. 35 (1996) 2171.
[54] S.J. Angyal, Adv. Carbohydr. Chem. Biochem. 49 (1991) 19.
[55] A. Al-Ajlouni, A. Bakac, J.H. Espenson, Inorg. Chem. 32 (1934) 5792.
[56] S. Muralidharan, J.H. Espenson, Inorg. Chem. 23 (1984) 636.

[57] J.K. Hurst, Free Radical Biol. Med. 53 (2012) 508.
[58] J.C. González, S. García, N. Mamana, L.F. Sala, S. Signorella, Inorg. Chem. Commun. 9 (2006) 437.
[59] J.C. González, S. García, S. Bellú, J.M. Salas Peregrín, A.M. Atria, L.F. Sala, S. Signorella, Dalton Trans. 39 (2010) 2204.
[60] G. Escandar, L. Sala, Can. J. Chem. 70 (1992) 2053.